Immune modulation by helminths and the impact on the development of type 2 diabetes

Ruiter, K. de

8

EFFECT OF DEWORMING ON TYPE 2 AND REGULATORY RESPONSES REVEALED BY MASS CYTOMETRY

Karin de Ruiter, Dicky L. Tahapary*, Koen A. Stam*, Vincent van Unen, Thomas Höllt, Boudewijn P.F. Lelieveldt, Frits Koning, Erliyani Sartono, Johannes W.A. Smit, Taniawati Supali and Maria Yazdanbakhsh

*Both authors contributed equally

Manuscript Submitted

ABSTRACT

Numerous studies have shown that helminths can have a profound role in shaping immune responses to vaccines, allergens or autoantigens, by inducing strong type 2 and regulatory responses, however, the degree of heterogeneity of such cells has not been studied before. Mass cytometry, which provides a method that allows in depth profiling of immune responses, was used to profile type 2 and regulatory immune cells in Europeans not exposed to helminth infections, and in Indonesians who were infected with soil-transmitted helminths (STH), before and 1 year after deworming. The use of Hierarchical Stochastic Neighbor Embedding (HSNE) in Cytosplore allowed the identification of very distinct immune signatures in Europeans and Indonesians, showing expanded frequencies of Th2 cells, in particular CD161$^+$ cells, and regulatory T cells, but only those expressing CTLA4 and co-expressing CD38, HLA-DR, ICOS or CD161, in STH-infected Indonesians. It was also possible to analyse ILC2s, which are difficult to study in peripheral blood, and to show that these cells are expanded in STH-infected Indonesians. The expansion of type 2 cells was confirmed functionally through analysis of type 2-cytokine producing cells, whereas IL-10 production alone could not capture the difference seen in regulatory T cells observed through phenotypic characterization. However, CD11c$^+$ B cells were the main IL-10 producers among B cells in Indonesians, a subset which was almost absent in Europeans. In addition to ILC2s and CD4$^+$ T cells, CD8$^+$ T cells as well as γδ T cells were found to be producers of type 2 cytokines in STH-infected Indonesians. A number of these expanded responses were shown to be driven by current helminth infection as they decreased following treatment and clearance of infection. These results provide us with a detailed insight into the types of cells that participate in strong type 2 and regulatory networks, and show that treatment of helminths affects specific groups of cells in these immune networks.

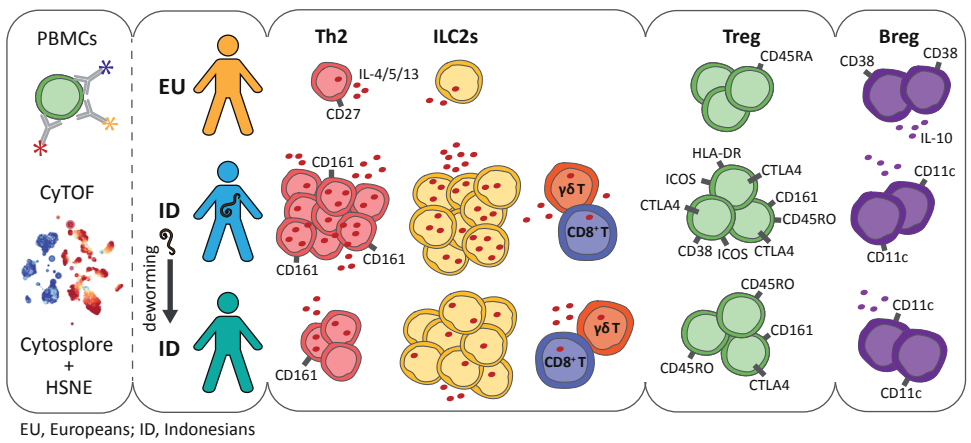

Graphical abstract

INTRODUCTION

Parasitic helminths represent one of the most prevalent infections affecting nearly one-third of the population worldwide (1), and are known as the strongest natural inducers of type 2 immune responses (2). These are characterized by CD4$^+$ T helper 2 (Th2) cells secreting the hallmark cytokines interleukin (IL)-4, IL-5 and IL-13, systemic and localized eosinophilia, expansion of basophils and mast cells, goblet cell hyperplasia and the production of IgE (3). There is evidence for a role of type 2 immune responses in controlling the number of parasites through direct killing or expulsion, and in inducing tissue repair, necessary to protect against damage caused by tissue-migrating helminths (4). In addition, an innate source of type 2 cytokines, termed group 2 innate lymphoid cells (ILC2s) described in both mice (5-7) and humans (8) are also part of the "type 2 immune system". Whereas murine ILC2s have been shown to contribute to anti-helminth immunity (5-7), information about their role in human helminth infections is lacking, and it has been challenging to study these cells considering their low frequency in peripheral blood (9).

Studies have shown that helminths can have a profound role in shaping immune responses to vaccines, allergens or autoantigens, and besides polarizing the immune system towards a strong type 2 immune response, their modulatory effects can be attributed to the induction of a strong regulatory network (2). Regulatory T cells (Tregs), expressing FOXP3, are an important component of such a network, and mediate their effects through cytokine-mediated suppression (e.g. IL-10 and TGF-β) and the expression of suppressory molecules such as cytotoxic T lymphocyte antigen 4 (CTLA4) (10). Several studies in animal models and humans show that helminth infections are associated with increased Treg frequencies and/or functional capacity (11-14). Although longitudinal studies assessing the effect of deworming on Tregs are rare, we recently found that not Treg frequencies, but the expression of CTLA4 on CD4$^+$ T cells significantly declined in anthelmintic-treated individuals (15).

To fully understand the diverse immune modulatory processes mediated by helminths and identify specific cells that might be important, we performed unbiased immune profiling of Indonesians residing in a rural area of Indonesia, who were infected with soil-transmitted helminths (STH), and 1 year after 3-monthly anthelmintic treatment, were free of these infections. Mass cytometry (Cytometry by time-of-flight; CyTOF) was applied, which allows high-resolution dissection of the cellular composition of the immune system by the simultaneous measurement of 37 cellular markers at the single-cell level.

A well-established technique for mass cytometry data analysis is t-distributed Stochastic Neighbour Embedding (t-SNE) (16), an algorithm that allows visualization of all concurrent marker expression profiles of cells on a two-dimensional plot in an unbiased fashion. However, t-SNE does not scale well to large amounts of data. Recently introduced techniques, such as Uniform Manifold Approximation and Projection (UMAP) (17) and Hierarchical Stochastic Neighbor Embedding (HSNE) (18) promise to overcome this scaling problem. Here, we applied HSNE, as implemented in Cytosplore (19), to visualize

and cluster the data. This allowed efficient visualization of our dataset containing 20 million cells without the need for downsampling of the data, while preserving single-cell resolution. These methods were applied to study the effect of helminths on the immune cell phenotype *ex vivo*, in addition to determination of functional effects in terms of cytokine production. Moreover, immune profiles were compared to those of healthy Europeans who had not been exposed to helminths.

MATERIALS AND METHODS

Study population

Samples in this study were part of the SugarSPIN trial, a household-based cluster-randomized double-blind trial that was conducted in three villages in Nangapanda, Ende district of Flores island (East Nusa Tenggara), Indonesia (20). The trial was approved by the ethics committee of Faculty of Medicine, Universitas Indonesia (FKUI) (ref: 549/H2·F1/ETIK/2013), and filed by the ethics committee of Leiden University Medical Center (LUMC). The trial is registered as a clinical trial (Ref: ISRCTN75636394). Written informed consent was obtained from participants prior to the study.

All subjects selected for the current study were infected with soil-transmitted helminths at baseline (Table 1), and cleared their infection after 1 year of albendazole treatment. The treatment consisted of a single tablet of albendazole (400 mg; PT Indopharma Pharmaceutical, Bandung, Indonesia) for three consecutive days, and this regimen was given every three months for a total of four rounds (maximum of 12 tablets in total), between May 2014 and February 2015. Before the start of drug administration and 6 weeks after the last round of drug administration, blood and stool samples were collected as previously described (20).

With regards to the European samples, we collected venous blood of 10 healthy volunteers who had not been exposed to helminths for PBMC isolation. Except for sex and age (Table 1), no additional data were collected.

Parasitology

Aliquots of fresh stool samples were frozen at -20°C in the field study centre and subsequently at -80°C at the Department of Parasitology of FKUI and LUMC for DNA extraction. Stool DNA isolation and real-time PCR were performed pairwise (baseline and follow-up). DNA isolation from stool was performed as described elsewhere (21). Multiplex real-time polymerase chain reaction (PCR) was performed to simultaneously detect the presence of hookworm (*Ancylostoma duodenale*, *Necator americanus*), *Ascaris lumbricoides*, *Trichuris trichiura*, and *Strongyloides stercoralis,* using a method described previously (21). Stool samples were considered positive by PCR when cycle threshold (Ct) values were <50.

Table 1. Characteristics of the study population.

Characteristic	Europeans (n=10)	Indonesians (n=10)
Age, years (median, min, max)	32.0 (26-55)	35.9 (18-56)
Sex, female, *n*	5	5
Eosinophil count, %, (GM, min, max)	na	13.7 (9-28)
Total IgE, IU/mL, (GM, min, max)	na	823 (124-7753)
Helminth infection by PCR, No.		
Single	na	5
Multiple		5

GM, geometric mean; na, not applicable

Eosinophil count and total IgE

A Giemsa-stained peripheral thin blood smear was read to assess the differential white blood cell count, resulting in a relative percentage of basophils, eosinophils, neutrophils, lymphocytes and monocytes. Total IgE was measured in serum as described previously (22).

PBMC cryopreservation

After diluting heparinised venous blood 2x with HBSS, PBMCs were isolated using Ficoll density gradient centrifugation within 12 hours after blood collection. The HBSS contained 100 U/mL penicillin G sodium and 100 µg/mL streptomycin. After washing twice with HBSS, the PBMCs were cryopreserved in RPMI 1640 containing 20% of heat-inactivated foetal calf serum (FCS; Bodinco, Alkmaar, the Netherlands) and 10% dimethyl sulfoxyde (DMSO). The RPMI medium contained 1 mM pyruvate, 2 mM L-glutamine, penicillin G and streptomycin. Cryovials containing the cell suspension were transferred to a Nalgene Mr Frosty Freezing Container (Thermo Scientific, Waltham, MA, USA) which was placed at a -80°C freezer for a minimum of 4 hours. Subsequently, vials were stored in liquid nitrogen until analysis. The cryopreserved PBMCs collected in the field were shipped in a liquid nitrogen dry vapour shipper from Jakarta, Indonesia, to Leiden, the Netherlands, for analysis.

Mass cytometry antibody staining

Two antibody panels were designed to 1) phenotype immune cells *ex vivo* and 2) assess cytokine production after 6 hours of stimulation with phorbol 12-myristate 13-acetate (PMA) and ionomycin. Details on antibodies used are listed in Supplementary table S1 and S2. Antibody-metal conjugates were either purchased or conjugated using a total of 100 µg of purified antibody combined with the MaxPar X8 Antibody Labelling Kit (Fluidigm, South San Francisco, CA, USA) according to manufacturer's protocol V7. The conjugated antibody was stored in 200 µL Antibody Stabilizer PBS (Candor Bioscience, GmbH, Wangen, Germany) at 4°C. All antibodies were titrated on study samples.

On the day of the staining, cryopreserved PBMCs were thawed with 50% FCS/RPMI medium at 37°C and washed twice with 10% FCS/RPMI medium. Next, $3x10^6$ cells per sample, used for phenotyping (Panel 1), were temporarily stored on ice while another $3x10^6$ cells per sample were transferred to 5 ml round-bottom Falcon tubes (BD Biosciences, Bedford, MA, USA) for 6 hours of incubation in 10% FCS/RPMI with 100 ng/mL PMA (Sigma; cat.P8139) and 1 µg/mL ionomycin (Sigma; cat. I0634). After 2 hours of incubation at 37°C, 10 µg/mL brefeldin A (Sigma; cat. B7651) was added after which the cells were incubated for 4 more hours. Subsequently, the cells were washed with PBS and resuspended in MaxPar staining buffer (Fluidigm) before continuing with the antibody staining (Panel 2).

For phenotyping (Panel 1), the staining was based on MaxPar Nuclear Antigen Staining Protocol V2 (Fluidigm). First, cells were washed with MaxPar staining buffer and centrifuged for 5 minutes at 300g in 5 mL eppendorf tubes. Then, the cells were incubated with 1 mL 500x diluted 500 µM Cell-ID Intercalator-103Rh (Fluidigm) in staining buffer at room temperature for 15 minutes to identify dead cells. After washing with staining buffer, cells were incubated with 5 µL Human TruStain FcX Fc-receptor blocking solution (BioLegend, San Diego, CA, USA) and 40 µL staining buffer at room temperature for 10 minutes. Then, 50 µL of freshly prepared surface antibody cocktail was added and incubated at room temperature for another 45 minutes. Subsequently, cells were washed 2x with staining buffer and fixed and permeabilized using the eBioscience FOXP3/Transcription factor staining buffer set (eBioscience, cat. 00-5523-00). After cells were incubated with 1 mL of the freshly prepared Fix/Perm working solution (prepared according to the manufacturer's instructions) for 45 minutes, cells were washed 2x with 1x Permeabilization buffer at 800g for 5 minutes. Next, 50 µL of the intranuclear antibody cocktail was added to 50 µL of cells resuspended in 1x Permeabilization buffer and incubated for 30 minutes at room temperature. Following the incubation, cells were washed once with 1x Permeabilization buffer and twice with staining buffer, before being stained with 1 mL 1000x diluted 125 µM Cell-ID Intercalator-Ir (Fluidigm) in MaxPar Fix and Perm buffer (Fluidigm) at 4°C overnight to stain all cells. After 3 washes with staining buffer and centrifugation at 800 g, cells were stored as a pellet at 4°C and measured within 2 days.

To assess the cytokine production of PBMCs (Panel 2), the staining was based on MaxPar Cytoplasmic/Secreted Antigen Staining Protocol V3. While the surface staining was performed exactly as described above, cells were afterwards fixed by incubating them with 1 mL of freshly prepared 1x MaxPar Fix I buffer (Fluidigm) for 20 minutes at room temperature. Next, cells were washed 3x with MaxPar Perm-S buffer (Fluidigm) and 50 µL of cytokine antibody cocktail was added to 50 µL of cell suspension and incubated for 40 minutes at room temperature. Then, cells were washed 3x with staining buffer and stained with Cell-ID Intercalator-Ir as described above.

Mass cytometry data acquisition

Measurement of samples was randomised per subject to avoid bias, but samples belonging to the same subject were stained and measured together. Samples were measured with a Helios™ mass cytometer (Fluidigm), which was automatically tuned according to Fluidigm's recommendations. Before measuring, cells were counted, washed with Milli-Q water, passed over a cell strainer, and brought to a concentration of $1.0x10^6$ cells/mL with 10% EQ Four Element Calibration Beads (Fluidigm) in Milli-Q water. Mass cytometry data were acquired and analysed on-the-fly, using dual-count mode and noise-reduction on. Next to channels to detect antibodies, channels for intercalators (103Rh, 191Ir, 193Ir), calibration beads (140Ce, 151Eu, 153Eu, 165Ho, and 175Lu) and background/contamination (133Cs, 138Ba, 206Pb) were acquired. After data acquisition, the mass bead signal was used to normalize the short-term signal fluctuations with the reference EQ passport P13H2302 during the course of each experiment. When applicable, normalized FCS files were concatenated using Helios software, without removing beads.

Mass cytometry data analysis

FlowJo V10 for Mac (FlowJo LLC, Ashland, OR, USA) was used to gate out beads and we discriminated live, single $CD45^+$ immune cells with DNA stain and event length. The selected cells were exported as FCS files and analysed using novel HSNE (18), as implemented in Cytosplore (19, 23). HSNE constructs a hierarchy of non-linear similarities that can be interactively explored with a stepwise increase in detail up to the single-cell level (19). Briefly, the data exploration starts with the visualization of the embedding at the highest level, the overview level, where the layout of the landmarks (representative cells) indicates similarity in the high-dimensional space. The landmark size reflects its area of influence (AoI), containing cells that are well-represented by the landmark, and the similarity of two landmarks is defined as the overlap of their respective AoIs. Colouring of the landmarks is used to represent marker expressions. At the overview level, a group of landmarks (also referred to as cluster) can be selected, by manual gating based on visual cues such as marker expression, or by performing unsupervised Gaussian mean shift (GMS) clustering (23, 24) of the landmarks based on the density representation of the embedding. Next, we can zoom into this selection by means of a more detailed embedding and visualize all selected landmarks in a next level. While this process can be repeated until the data level is reached where each dot represents a single cell, this is not imperative and we often clustered at an intermediate level without reaching the data level. The number of hierarchical levels depended on the input-data size.

Before HSNE was applied, data were transformed using a hyperbolic arcsin with a cofactor of 5. Furthermore, within Cytosplore, an extra channel called 'SampleTag' was added to the FCS files to be able to identify from which sample an event originated after HSNE.

Clusters produced in Cytosplore were analysed using R software (R x64 version 3.5.1; R Foundation for Statistical Computing, Vienna, Austria, http://www.r-project.org/) and RStudio (Rstudio, Inc., Boston, MA, USA, www.rstudio.com). The package 'cytofast' was used to produce heatmaps, scatterplots showing subset abundance and histograms showing the median signal intensity distribution of markers (25).

Statistical Analysis

Statistical analyses were performed using R software. To compare subpopulation and cluster abundance between Europeans and Indonesians pre-treatment unpaired *t* tests were used. Paired *t* tests were applied to compare pre- and post-treatment samples of Indonesians. Total IgE levels and eosinophil counts were log-transformed for analysis and paired *t* tests were used in GraphPad Prism (GraphPad Software, San Diego, CA, USA). Spearman's correlation was used to assess the relationship between the frequency of Tc2 cells and type 2 cytokine-producing CD8$^+$ T cells. *P* values <.05 were considered statistically significant.

RESULTS

Distinct immune signatures between Europeans and Indonesians

Study population characteristics are shown in Table 1. To analyse the cellular composition of the immune system at high-resolution, we developed a 37-metal isotope-tagged monoclonal antibody panel (Table S1) which allowed the identification of the six major immune lineages (CD4$^+$, CD8$^+$, γδ T cells, B cells, myeloid cells and innate lymphoid cells (ILCs; CD3$^-$CD7$^+$)), and major subpopulations and detailed cell clusters within. Importantly, by using the t-SNE-based HSNE (19), we could explore the full mass cytometry dataset containing 20.3 million live CD45$^+$ cells at the single-cell level without the need for downsampling. At the overview level, landmarks (representative cells) depict the global composition of the entire immune system and distinguished the major immune lineages, which were annotated based on lineage marker expression overlays (Fig. 1A-B). Quantification of cell frequencies revealed a significantly higher frequency of B cells in Indonesians (*P* = .03), but no other differences were found between Europeans and Indonesians at the lineage level (Fig. 1C, Fig. S1). Next, CD4$^+$ T cell landmarks, representing 6.3 million cells, were selected at the overview level (Fig. 1B) and a new higher resolution embedding was generated at the second level of the hierarchy (Fig. 1D), revealing subpopulations within the CD4$^+$ T cell lineage (Fig. 1D). Stratification by origin of the samples revealed a strikingly different distribution of the CD4$^+$ T cells between European and Indonesian individuals, visualized by cell density plots (Fig. 1E). Different cellular distributions were also observed within other lineages (CD8$^+$, γδ T cells, B cells, myeloid cells and ILCs) (Fig. 1E), suggesting distinct immune signatures between Europeans and Indonesians in both the innate and adaptive immune compartment.

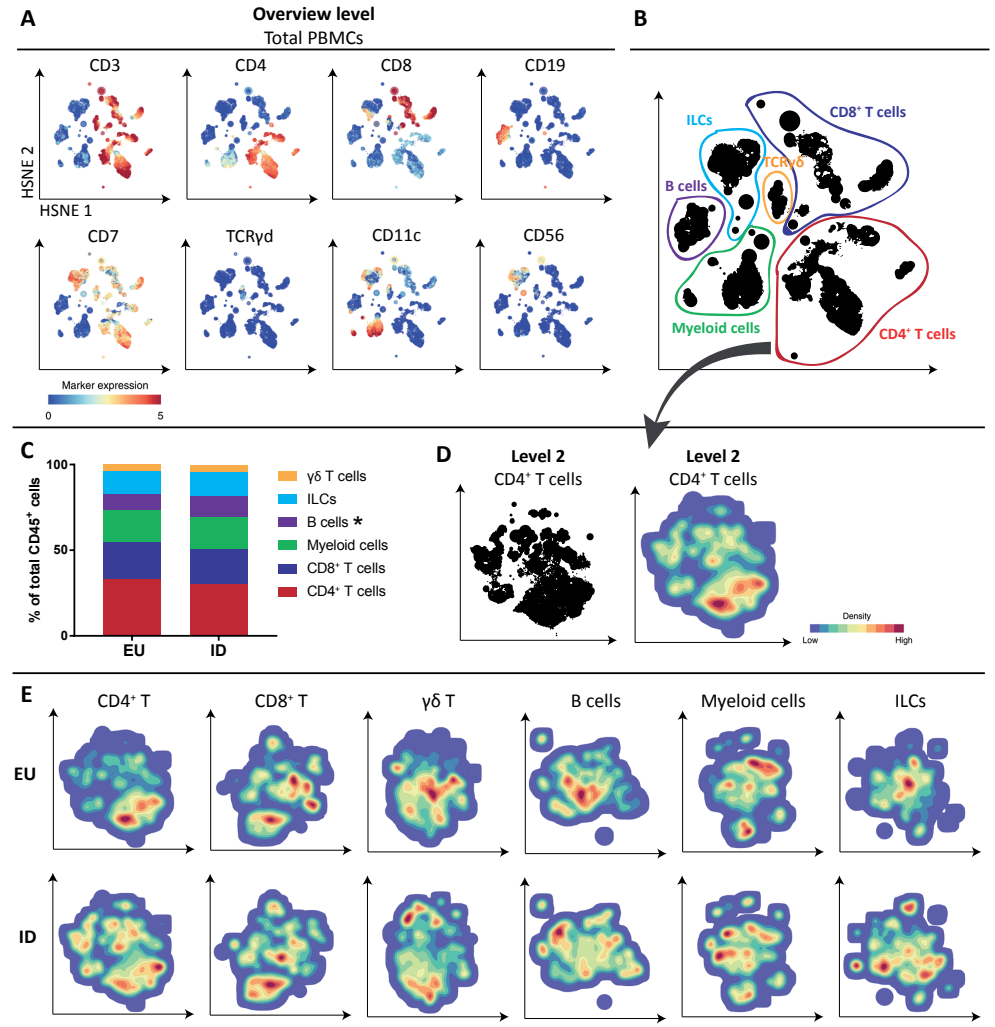

Figure 1. Distinct immune signatures between Europeans and Indonesians. A. First HSNE level embedding of 20.3 million cells. Colour represents arsin5-transformed marker expression as indicated. Size of the landmarks represents AoI. **B.** The major immune lineages, annotated on the basis of lineage marker expression. **C.** Comparison of lineage proportions relative to total cells between Europeans (EU) and Indonesians (ID). Differences between EU and ID were tested with Student's *t* test. **P* <.05. **D.** Second HSNE level embedding of the CD4$^+$ landmarks selected from the overview level of total PBMCs, as indicated by the red encirclement. Both landmarks (left panel) and the density features of the CD4$^+$ T cells (right panel) are shown. Density is indicated by colour. **E.** Density plots per lineage, stratified by sample origin, and therefore illustrating the differences between EU and ID.

A CD161⁺ subpopulation of Th2 cells is expanded in Indonesians and decreases after anthelmintic treatment

Within the CD4⁺ T cells, a distinct population of Th2 cells was found that expressed GATA3, CD25, CD127, CD45RO and chemoattractant receptor-homologous molecule expressed on Th2 (CRTH2), the latter being the most reliable marker to identify human Th2 cells (26) (Fig. 2A). The frequency of total Th2 cells was significantly higher in Indonesians compared to Europeans (*P* = .003) and importantly, deworming resulted in a significant decrease (*P* = .008) (Fig. 2B). This is in line with the observation that the proportion of circulating eosinophils as well as serum levels of total IgE, both markers of the type 2 response, significantly decreased in the STH-infected Indonesian individuals after treatment (Fig. S2).

Further analysis of Th2 cells revealed 22 phenotypically distinct clusters using the GMS clustering (Fig. 2C) and generated a heatmap showing the distinct marker expression profiles for each cluster (Fig. 2G). Th2 cells were found to be heterogeneous and based on the expression of the lectin-like receptor CD161 and CD27, the latter which is lost on highly differentiated memory CD4⁺ T cells (27, 28), three subpopulations could be identified (CD161⁺CD27⁻, CD161⁻CD27⁻ and CD161⁻CD27⁺ Th2 cells; Fig. 2C-D). Visualization of Th2 cells by density plots (Fig. 2E) showed that the proportion of CD161⁺ Th2 cells was expanded in Indonesians compared to Europeans, although the difference fell short of statistical significance, but a significant decrease was observed after anthelmintic treatment (*P* = .01) (Fig. 2F). Deeper analysis at the cluster level revealed three clusters within the CD161⁺ Th2 population that significantly declined upon deworming, characterized as CD161⁺CD7⁻ KLRG1⁻, CD161⁺CD7⁻KLRG1⁺ and CD161⁺CD7⁺KLRG1⁻ (Fig. 2G). In contrast, after one year of treatment we observed a significant increase of three CD7⁺ Th2 clusters that only weakly expressed GATA3 and CRTH2 (Fig. 2G).

Although Indonesian blood samples contained more Th2 cells, the proportion of poorly differentiated CD27⁺ Th2 cells was significantly higher in Europeans (*P* = .019) (Fig. 2F) and this difference was in particular seen in the CCR7⁻ cluster within the CD27⁺ Th2 cell subpopulation (Fig. 2G). This finding indicates the relatively low presence of highly differentiated memory effector Th2 cells in the immune system of Europeans.

Overall frequency of ILC2s is expanded in Indonesians but does not decrease after anthelmintic treatment.

When 2.8 million ILCs (CD3⁻CD7⁺), which include NK cells and helper-like ILCs, were analysed at a more detailed level, the embedding of a CD25⁺CD127⁺CD161⁺ subpopulation revealed 2 distinct clusters that were phenotyped as ILC2s and ILC3s, based on the expression of CRTH2 and c-Kit, respectively (Fig. 3A). It was found that other markers such as GATA3, KLRG1, CD45RA and CCR6 could also be expressed by ILC2s and/or ILC3s (Fig. 3A). Consistent with previous work (29), we observed that while GATA3, the Th2 master transcription factor, was highly expressed in CRTH2⁺ ILC2s, it was also expressed in CRTH2⁻ ILCs and can therefore not exclusively be used to define ILC2 cells.

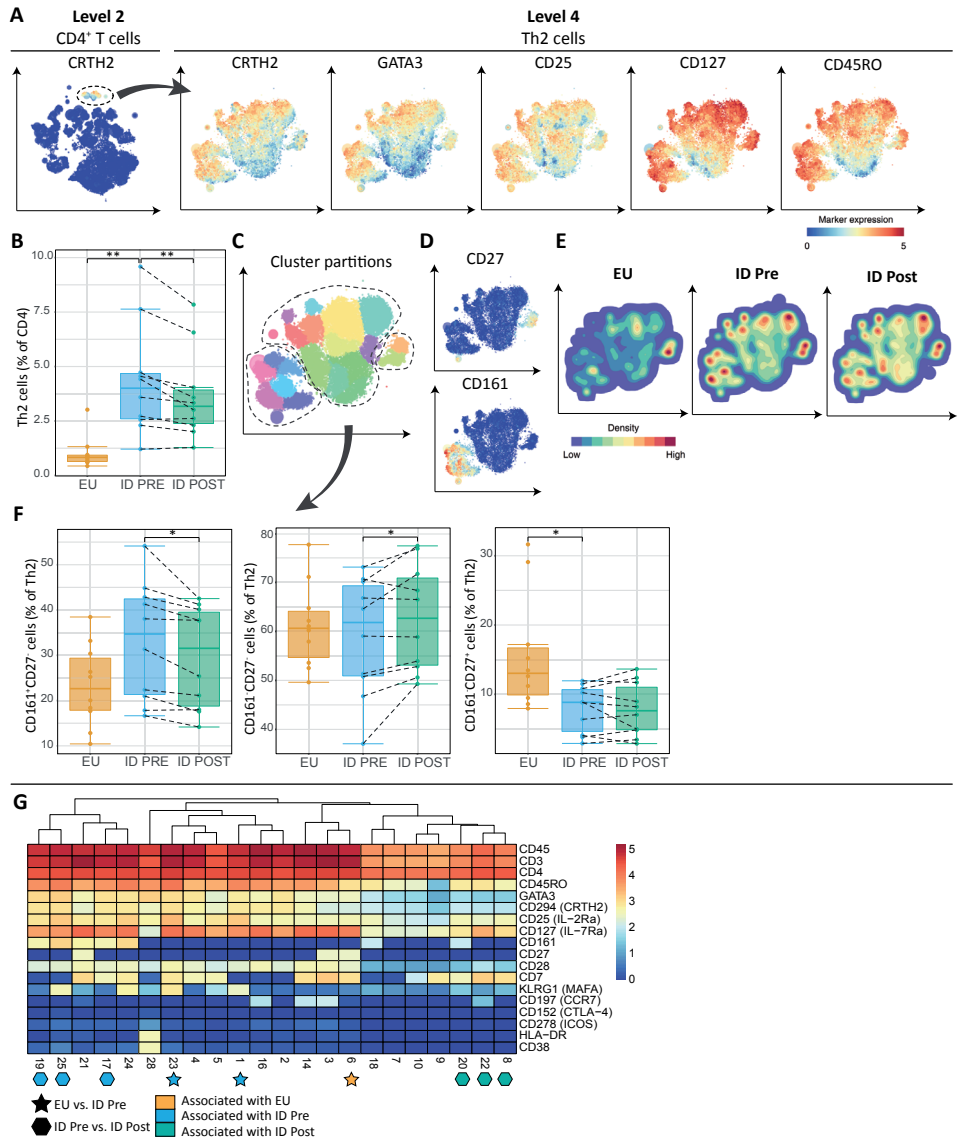

Figure 2. A CD161⁺ subpopulation of Th2 cells is expanded in Indonesians and decreases after anthelmintic treatment. A. Fourth HSNE level embedding of the CRTH2⁺ landmarks (Th2 cells) selected from the second HSNE level embedding of 6.3 million CD4⁺ T cells, as indicated by the black encirclement. Colour represents arsin5-transformed marker expression as indicated. Size of the landmarks represents AoI. **B.** Frequency of Th2 cells relative to CD4⁺ T cells. Differences between Europeans (EU) and Indonesians pre-treatment (ID Pre) were tested with Student's *t* test, while differences between ID Pre and ID Post were assessed using paired *t* tests. ***P* <.01. **C.** Cluster partitions of Th2 cells using density-based GMS clustering. The black encirclement indicates three subpopulations, whose frequencies are shown in f. **D.** Marker expression of CD27 and CD161 on Th2 cells. **E.** Density features of Th2 cells illustrating the different distribution of cells between EU, ID Pre and ID Post. **F.** Frequency of three Th2 subpopulations (CD161⁺CD27⁻, CD161⁻CD27⁻, CD161⁻CD27⁺) relative to total Th2 cells. **P* <.05. **G.** A heatmap summary of median expression values (same colour ▸

coding as for the embeddings) of cell markers expressed by CRTH2⁺ clusters identified in c. and hierarchical clustering thereof. To compare cluster abundance between EU and ID Pre Student's *t* test was used, while paired *t* test was used to compare ID Pre and ID Post. Coloured symbols below the clusters indicate statistical significance.

In contrast to ILC3s, the proportion of ILC2s was significantly higher in Indonesians compared to Europeans (P = .003), and did not change after anthelmintic treatment (Fig. 3B). Further characterization of ILC2s resulted in 8 phenotypically distinct clusters that were mainly distinguished by the expression of KLRG1, CD45RA and CCR6 (Fig. 3C). Except for a higher frequency of KLRG1⁺CCR6⁻ ILC2s (cluster 2) present in STH-infected Indonesians and a lower frequency of KLRG1⁺CCR6⁺ ILC2s (cluster 5) compared to Europeans, no significant differences at the cluster level were observed (Fig. 3D).

Not Treg frequency, but their expression of CTLA4 is induced by helminth infections

Regulatory T cells (Tregs) were characterized as FOXP3⁺CD25^{high}CD127^{low} cells and appeared as a clearly distinct subpopulation within CD4⁺ T cells (Fig. 4A). The frequency of Tregs, when assessed as a whole, did not differ between Europeans and Indonesians, nor changed after deworming (Fig. 4B). However, the immune profile of Indonesians consisted of significantly more effector Tregs expressing CD45RO (P = .036) (Fig. 4C), whereas in Europeans, a clear population of Tregs was positioned in the naïve, CD45RA⁺, compartment (Fig. 4A,D). In line with previous studies describing Tregs as phenotypically and functionally heterogeneous (10), we found several subpopulations within the effector Treg compartment expressing CTLA4, HLA-DR, CD38 and/or ICOS (Fig. 4E). A significant proportion of the effector Tregs expressed CTLA4, a marker that is associated with the suppressive function of Tregs (30). In concordance with this, the proportion of CTLA4⁺ Tregs was significantly higher in Indonesians compared to Europeans (P = .007) and decreased after treatment (P = .052) (Fig. 4F).

Next, we identified 27 phenotypically distinct clusters within Tregs (Fig. 4G-H). Analysis at the cluster level revealed that the frequencies of 6 out of 27 clusters were significantly higher in Indonesians compared to Europeans, which could be distinguished by the expression of only CTLA4⁺, or co-expressing CD38 and/or HLA-DR and/or ICOS (Fig. 4H). One of these clusters (cluster 7) expressing CTLA4, HLA-DR, CD38 and ICOS decreased significantly upon deworming, suggesting that this population of effector Tregs is particularly important in the immune response induced by STH.

Of note, among the CTLA4⁺ Tregs, we identified a cluster expressing CD161 (cluster 25; Fig. 4H), characterizing a subpopulation that was previously described as the major source of Treg-derived proinflammatory cytokines with the ability to produce IL-17 under inflammatory conditions (31, 32). The proportion of CD161⁺ Tregs was significantly higher in Indonesians compared to Europeans (P = .001) but did not change after deworming (Fig. 4I).

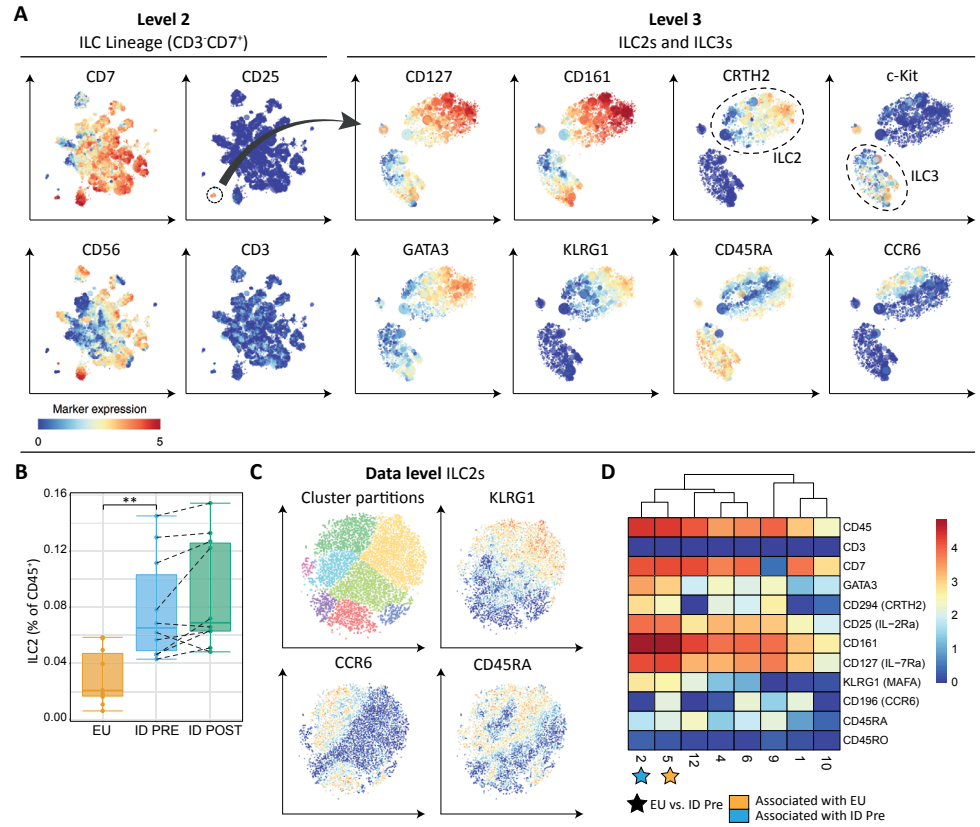

Figure 3. Overall frequency of ILC2s is expanded in Indonesians but does not decrease after anthelmintic treatment. A. The right panel shows the third HSNE level embedding of the CD25⁺CD161⁺CD127⁺ landmarks selected from the second HSNE embedding of 2.8 million ILCs (CD3⁻CD7⁻), as indicated by the black encirclement. Next to a distinct cluster of CRTH2⁺ ILC2s, a cluster of cKit⁺ ILC3s was found. Colour represents arsin5-transformed marker expression as indicated. Size of the landmarks represents AoI. **B.** Frequency of ILC2s relative to total CD45⁺ cells. Differences between Europeans (EU) and Indonesians pre-treatment (ID Pre) were tested with Student's *t* test, while differences between ID Pre and ID Post were assessed using paired *t* tests. ***P* <.01. **C.** Data level embedding of ILC2s. The upper left panel shows the cluster partitions using GMS clustering, whereas the other panels show the expression of KRLG1, CCR6 and CD45RA. **D.** A heatmap summary of median expression values (same colour coding as for the embeddings) of cell markers expressed by ILC2 cell clusters identified in c. and hierarchical clustering thereof. To compare cluster abundance between EU and ID Pre Student's *t* test was used, while paired *t* test was used to compare ID Pre and ID Post. Coloured symbols below the clusters indicate statistical significance.

Type 2 cytokine-producing cells in Indonesians (ILC2s, CD4⁺, CD8⁺ and γδ T cells) and their alteration after deworming

Following the phenotypic characterization of the cells, the cytokine-producing capacity of the cells was analysed to assess functional type 2 immune cells. PBMCs from identical donors as described above, were stimulated with PMA/ionomycin for 6h and subsequently

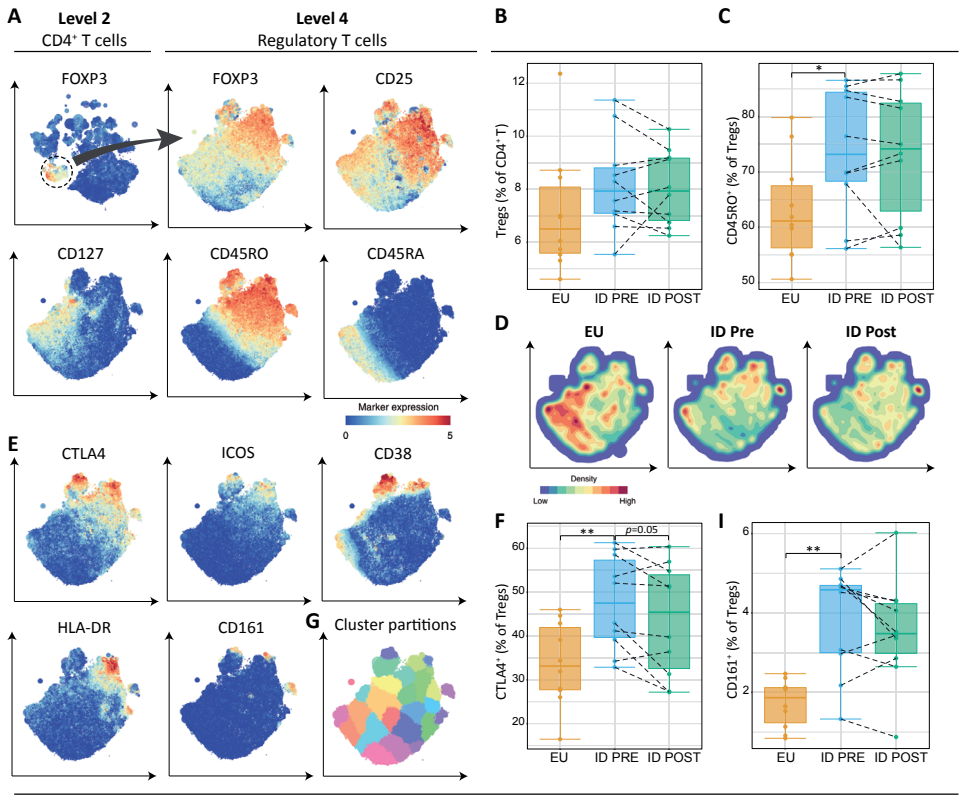

Figure 4. Not Treg frequency, but their expression of CTLA4 is induced by helminths. A. Fourth HSNE level embedding of the FOXP3⁺ landmarks (Tregs) selected from the second HSNE embedding of 6.3 million CD4⁺ T cells, as indicated by the black encirclement. Colour represents arsin5-transformed marker expression as indicated. Size of the landmarks represents AoI. **B.** Frequency of Tregs relative to CD4⁺ T cells. Differences between Europeans (EU) and Indonesians pre-treatment (ID Pre) were tested with Student's *t* test, while differences between ID Pre and ID Post were assessed using paired *t* tests. **C.** Frequency of CD45RO⁺ effector Tregs relative to total Tregs. **P* <.05. **D.** Density features of Tregs illustrating the different distribution of cells between EU, ID Pre and ID Post. **E.** Marker expression of CTLA4, ICOS, CD38, HLA-DR and CD161 by Tregs. **F.** Frequency of CTLA4⁺ Tregs relative to total Tregs. **P* <.05; ***P* <.01. **G.** Treg cluster partitions using GMS clustering. **H.** A heatmap summary of median expression values (same colour coding as for the embeddings) of cell markers expressed by FOXP3⁺ Treg clusters identified in g. and hierarchical clustering thereof. To compare cluster abundance between EU and ID Pre Student's *t* test was used, while paired *t* test was used to compare ID Pre and ID Post. Coloured symbols below the clusters indicate statistical significance. **I.** Frequency of CD161⁺ Tregs relative to total Tregs. **P* <.05.

stained with a 37-metal isotope-tagged monoclonal antibody panel which included the following cytokine antibodies: IFNγ, TNFα, IL-2, IL-17, IL-10 and IL-4/IL-5/IL-13 (simultaneously assessed and hereafter referred to as 'type 2 cytokines').

Type 2 cytokine-producing CD45⁺ cells were analysed in Cytosplore and clustering on surface markers clearly revealed four distinct type 2 cytokine-producing subpopulations (Fig. 5A-D, Fig. S3). Th2 cells and ILC2s have been described as the main producers of type 2-cytokines, and this was confirmed by the finding that the median signal intensity (MSI) of type 2 cytokines was highest in CD4⁺ T cells and ILC2s (Fig. 5E). However, we also identified a cluster of γδ T cells and multiple CD8⁺ T cell clusters producing type 2 cytokines, although the MSI of IL-4/5/13 was lower compared to CD4⁺ T and ILC2 cells (Fig. 5E). Interestingly, whereas ILC2s did not produce IFNγ, a CD25⁻ proportion of CD4⁺ and CD8⁺ T cells, and all γδ T cells co-expressed IFNγ (Fig. 5E-F).

Density plots of type 2 cytokine-producing cells revealed striking differences between Europeans and STH-infected Indonesians (Fig. 5C). While Indonesians not only exhibited a significantly higher frequency of type 2 cytokine-producing cells (Fig. 5G), the number of cellular sources for these cytokines also appeared to be expanded (Fig. 5C-D,H). In both populations it were mainly CD4⁺ T cells that produced type 2 cytokines, however, the ILC2 and γδ T cell subpopulations that were found in Indonesians, were much less pronounced in Europeans. Importantly, the proportion of type 2 cytokine-producing cells significantly declined after deworming ($P < .001$) (Fig. 5G) and this can be attributed to a significant decrease in type 2 cytokine-producing CD4⁺ T ($P < .001$) and ILC2s ($P = .004$) (Fig. 5H).

When cells were phenotyped *ex vivo*, we identified a GATA3⁺ cluster (2.1% of CD8⁺ T cells) within a subpopulation of CD45RO⁺CCR7⁻CD161⁻CD56⁻ CD8⁺ T cells (Fig. 6A-B), a subset previously defined as type 2 cytotoxic T cells (Tc2) cells (33, 34). In addition, Tc2 cells expressed CRTH2, CD25, CD127 and CD7 (Fig. 6B). Although Tc2 frequencies did not change after deworming, its proportion correlated strongly with the type 2 cytokine-producing CD8⁺ T cells (r=0.87, $P < .001$; Fig. 6C), suggesting that Tc2 cells are the source of Th2 cytokines within the CD8 lineage. However, it should be noted that the frequency of Tc2 cells ranged widely from 0.09-16.8% of CD8⁺ T cells among individuals, and 56% of the cells within the Tc2 subpopulation were from one individual (including both before and after treatment samples).

IL10-producing B and CD4⁺ T cells revealed by mass cytometry

Similar to what was described above, we sought cells that produced the suppressory cytokine IL-10. The IL-10-producing CD45⁺ cells were analysed in Cytosplore

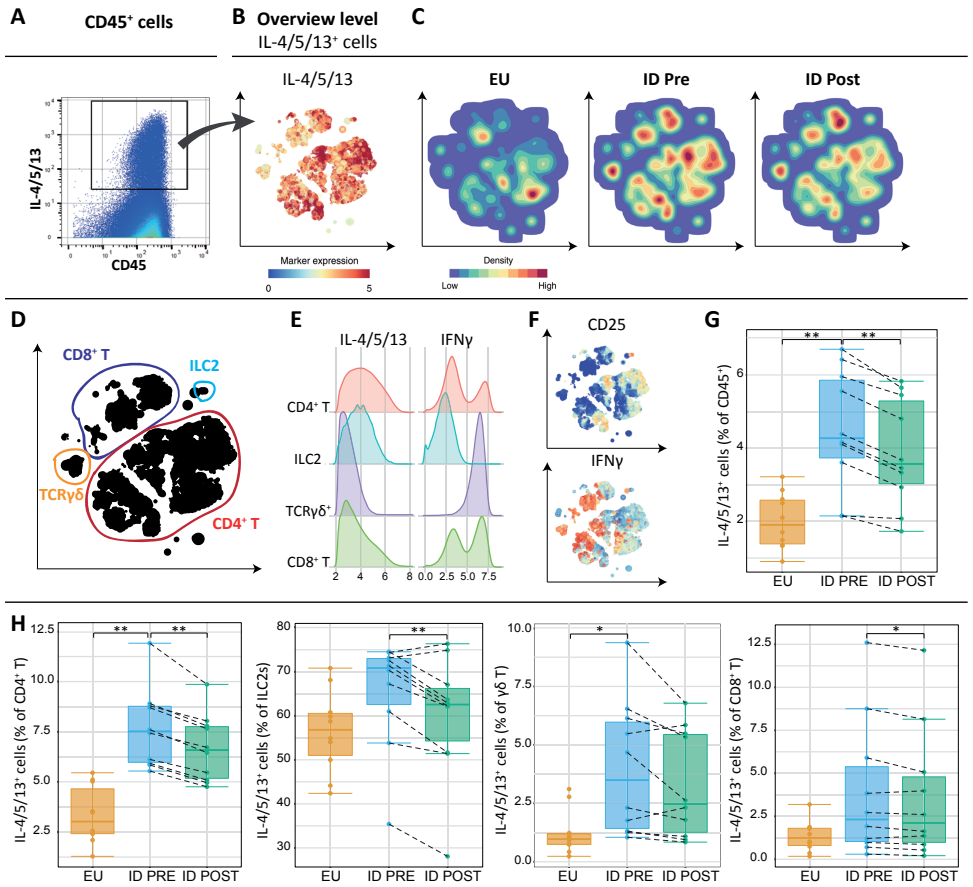

Figure 5. Type 2 cytokine-producing cells in Indonesians (ILC2s, CD4⁺, CD8⁺ and γδ T cells) and their alteration after deworming. A. IL-4/5/13⁺ cells were manually gated using Flowjo. Data from one representative individual is shown. **B.** First HSNE level embedding of total IL-4/5/13⁺ cells, clustered on surface markers. Colour represents arsin5-transformed marker expression as indicated. Size of the landmarks represents AoI. **C.** Density features of IL-4/5/13⁺ cells illustrating the different distribution of cells between Europeans (EU), Indonesians pre- (ID Pre) and post-treatment (ID Post). **D.** The major immune cell subpopulations producing type 2 cytokines, annotated on the basis of lineage marker expression (*See Fig. S3*). **E.** Histogram showing the median signal intensity (MSI) distribution of IL-4/5/13 and IFNγ for the subpopulations identified in d. **F.** Marker expression of CD25 and IFNγ by IL-4/5/13⁺ cells. **G.** Frequency of total IL-4/5/13-producing cells relative to total CD45⁺ cells. Differences between EU and ID Pre were tested with Student's *t* test, while differences between ID Pre and ID Post were assessed using paired *t* tests. ***P* <.01. **H.** Frequency of IL-4/5/13-producing clusters identified in d. relative to total CD4⁺ T, ILC2, γδ T or CD8⁺ T cells. **P* <.05; ***P* <.01.

(Fig. 7A-B) and clustering on surface markers revealed a major cluster of CD4⁺ T cells, and minor clusters of CD8⁺ T cells, CD4⁻CD8⁻ T cells and B cells (Fig. 7C-D, Fig. S4). Similar frequencies of total IL-10-producing cells (relative to CD45⁺ cells) were observed among Europeans and Indonesians, and these did not change after anthelmintic treatment (data

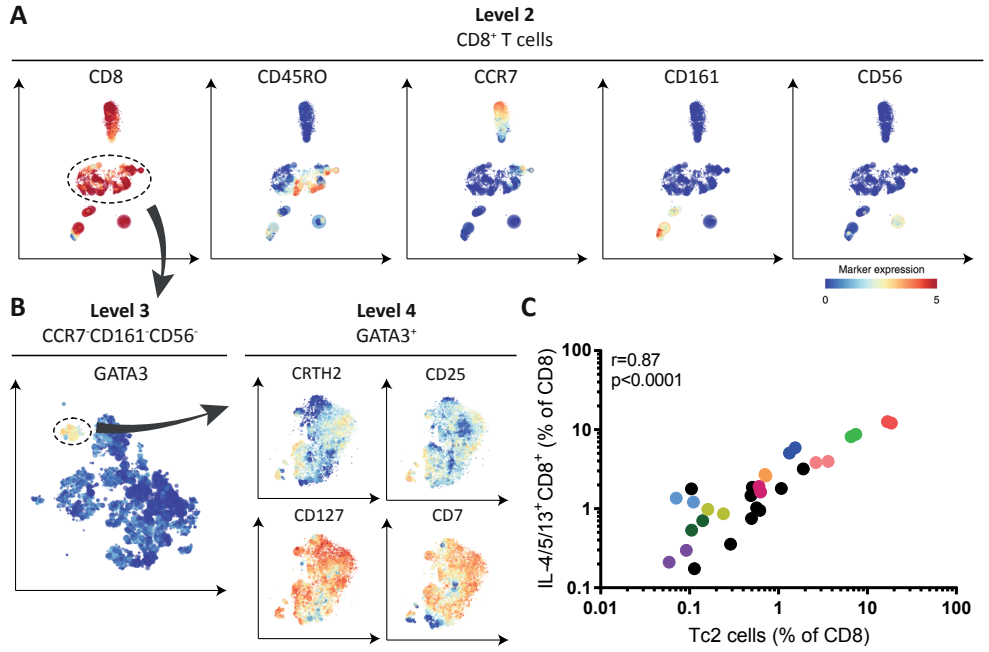

Figure 6. Tc2 cells are the source of type 2 cytokines produced by CD8⁺ T cells. A. CCR7⁻CD161⁻CD56⁻ landmarks were selected from the second level HSNE embedding of CD8⁺ T cells, as indicated by the black encirclement. **B.** From the next level embedding, GATA3⁺ landmarks were selected and their marker expression is shown at the fourth level embedding. Colour represents arsin5-transformed marker expression as indicated. Size of the landmarks represents AoI. **C.** Correlation of GATA3⁺CD8⁺ T (Tc2) cells identified in b. and IL-4/5/13-producing CD8⁺ T cells identified in Fig. 5D. Colours indicate paired samples (pre and post treatment) from Indonesian individuals. Spearman's rank correlation was used for statistical analysis.

not shown). Also regarding the IL-10⁺ subpopulations (CD4⁺, CD8⁺, CD4⁻CD8⁻ T and B cells), no significant differences were found (data not shown).

Interestingly, a distinct population of IL-10⁺ B cells (0.5% of total B cells) was identified and further analysis showed that it consisted of three clusters, namely CD11c⁺CD38⁻, CD11c⁻CD38⁺ and CD11c⁻CD38⁻ cells (Fig. 7E). Whereas the composition of IL-10⁺ B cells did not change after deworming, IL-10⁺ B cells from Indonesians clearly contained more CD11c⁺CD38⁻ cells compared to Europeans, who had relatively more CD11c⁻CD38⁺ IL-10⁺ B cells (Fig. 7F). These results indicate a different phenotype of IL-10⁺ B cells in the two populations, which is in line with the finding that the immune system of Indonesians contained significantly more CD11c⁺ B cells as assessed by phenotypic markers compared to Europeans (data not shown).

When IL-10-producing CD4⁺ T cells were clustered on cytokines, four clusters were identified which all expressed type 2 cytokines but varied in terms of co-expression of other cytokines (IFNγ, TNFα, and/or IL-2) (Fig. 7G-H). When considering all CD4⁺ T cells producing IL-10 and type 2 cytokines, irrespective of other cytokines, their frequency was

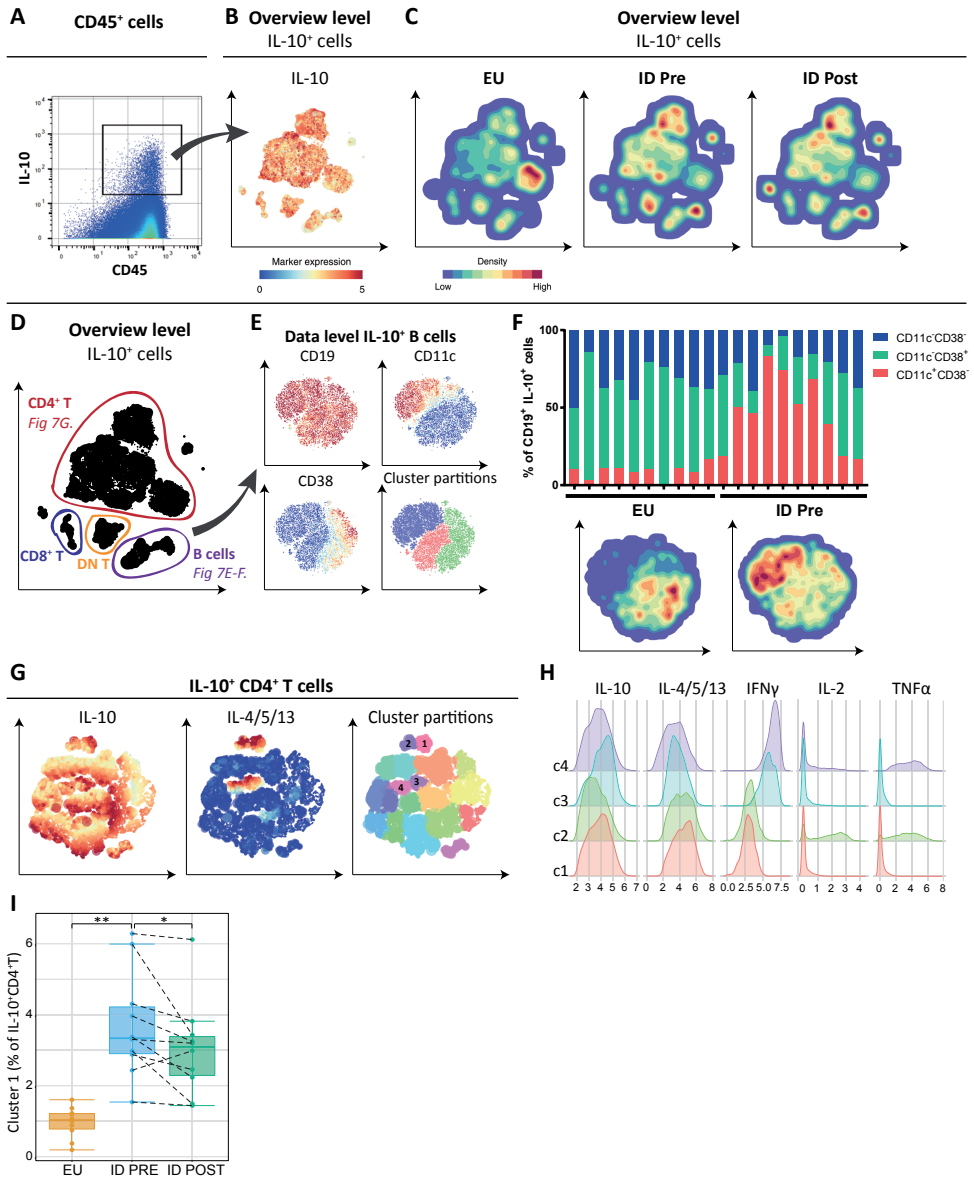

Figure 7. IL-10-producing B and CD4⁺ T cells revealed by mass cytometry. A. IL-10⁺ cells were manually gated using Flowjo. Data from one representative individual is shown. **B.** First HSNE level embedding of total IL-10⁺ cells, clustered on surface markers. Colour represents arsin5-transformed marker expression as indicated. Size of the landmarks represents AoI. **C.** Density features of IL-10⁺ cells illustrating the different distribution of cells between Europeans (EU), Indonesians pre- (ID Pre) and post-treatment (ID Post). **D.** The major immune cell subsets producing IL-10, annotated on the basis of lineage marker expression (*See Fig. S4*). **E.** Data level embedding of IL-10⁺ B cells and the cluster partitions using GMS clustering (lower right panel). **F.** Relative composition of IL-10⁺ B cells, comparing EU and ID Pre. Below, density features of IL-10⁺ B cells are shown illustrating the different distribution of cells between EU and ID Pre. **G.** First level HSNE embedding of IL-10⁺CD4⁺ landmarks selected in d. and clustered on cytokines. Four IL-4/5/13⁺ clusters were identified as indicated in the right panel showing the cluster partitions. **H.** Histograms showing the median signal intensity (MSI) distribution of cytokines for the four clusters identified in g. **I.** Frequency of cluster 1, co-expressing IL-4/5/13 and IL-10 (identified in g), relative to total IL-10-producing CD4⁺ T cells. Differences between EU and ID Pre were tested with Student's *t* test, while differences between ID Pre and ID Post were assessed using paired *t* tests. **P* <.05; ***P* <.01.

significantly higher in Indonesians compared to Europeans (*P* < .001; data not shown). However, only the cluster that was negative for IFNγ, TNFα, and IL-2 (cluster 1) decreased significantly after deworming (*P* = .041; Fig. 7I).

DISCUSSION

There are large population differences in immune responses that, although in part can be explained by genetic factors, seem to be largely driven by environmental exposures (35). One such exposure is to helminths, that are ubiquitous in many parts of the world. These parasites induce strong type 2 and regulatory responses and can shape vaccine efficacy or influence the development of inflammatory diseases. By understanding these responses in depth it will be possible to devise interventions that could help vaccine responses or curtail inflammation that damages tissues and organs. To this end, mass cytometry was applied to analyse type 2 and regulatory immune cells of healthy Europeans, as well as of STH-infected Indonesians before and one year after deworming, thereby starting to understand the differences in the immune response of populations living in different geographical areas.

Here, we have identified and shown the enhanced presence of Th2 and ILC2 cells, both sources of the type 2 cytokines IL-4, IL-5 and IL-13, in STH-infected Indonesians compared to Europeans. When considering the cells by their phenotype, Th2 cell frequencies significantly decreased after deworming, but the frequencies of ILC2s remained unchanged. However, the frequency of ILC2s producing type 2 cytokines declined after anthelmintic treatment, indicating decreased functional ILC2 activity. There is very little known about the role of ILC2s in human helminth infections. Although the identification of CRTH2 as a marker of human ILC2s (8) has been a great advantage, only two studies have analysed ILC2s in the context of human helminth infections (36, 37). In a cross-sectional study, Boyd et al. found a higher frequency of c-Kit⁺ ILCs (reported as Lin⁻CD45⁺CD127⁺) in filarial-infected adults (36), however, c-Kit⁺ ILCs have been described to contain both ILC2s and ILC3s (38), and here we did not detect c-Kit⁺ ILC2s. Another study showed that the proportions of ILC2s (reported as Lin⁻CD45⁺CD127⁺CRTH2⁺CD161⁺), when expressed as percentage of Lin⁻CD45⁺CD127⁺ cells, were significantly lower in *Schistosoma haematobium*-infected African children (6-9 years) when compared to age and sex matched uninfected individuals and increased 6 weeks after clearing the infection (37). In our study, when based on phenotypic characterization, there was a tendency for ILC2 frequencies to be higher (although not statistically significant) after deworming. However, decreased functional ILC2 activity in terms of cytokine production was observed and as this study did

not analyse the cytokine production by the cells, it is difficult to compare it with our data. As suggested by the authors (37), the reduction observed in infected individuals might be a consequence of ILC2s migrating and accumulating at the site of infection, or a decline in the generation or maintenance of the cells.

Unlike ILC3s, only one (functional) subset of ILC2s has been characterized in healthy humans (38). We identified 8 ILC2 clusters based on the heterogeneous expression of KLRG1, CD45RA and CCR6, but the significance of these is currently unknown and requires further investigation. Interestingly, we identified CD45RA$^+$c-Kit$^+$ ILC3s that did not express CCR6, a marker previously described to be expressed by ILC3s (29, 38), and hypothesize that this subpopulation might consist of the recently described ILC precursors (ILCPs), as these cells lack CCR6 expression and are CD45RA$^+$ (39).

There is increasing evidence that Th2 cells can be heterogeneous. For example, a minority subpopulation of Th2 cells termed pathogenic effector Th2 (peTh2) cells, found in patients with allergic eosinophilic inflammatory diseases, have been described that have enhanced effector function (27, 40). PeTh2 cells are characterized as CD161$^+$hPGDS$^+$CD27$^-$ Th2 cells, expressing IL-5 in addition to IL-4 and IL-13 and respond to innate stimuli including IL-25, IL-33 and TSLP indicating that they have innate-like properties (27). Although chronic antigen exposure is thought to drive peTh2 differentiation from conventional Th2 cells, it is unknown whether peTh2 cells are induced by or play a role in human helminth infections (27). Anarudha et al. previously identified IL-5$^-$IL-4$^+$IL-13$^+$ and IL-5$^+$IL-4$^+$IL-13$^+$ human CD4$^+$ T cell subpopulations in the context of filariasis, but the expression of CD161 was not assessed (41). Here, we describe the enhanced presence of a peTh2-like CD27$^-$ CD161$^+$ subset of Th2 cells in STH-infected individuals which significantly decreased after deworming. However, whether these cells are identical to peTh2 cells needs to be investigated in future studies.

Unlike Th2 cells, Tregs have been described as a heterogeneous population and previous work showed that HLA-DR (42), ICOS (43) and CD38 (44) are differentially expressed within the FOXP3$^+$ Treg population, marking cells with distinct capacities and modes of suppression. While Tregs expressing HLA-DR or CD38 were shown to be highly suppressive compared to their negative counterparts (42, 44), the expression of ICOS seems to define a Treg subset that has the capacity to produce large amounts of IL-10, in contrast to ICOS$^-$ Tregs producing mainly TGF-β (43). By using mass cytometry, we could not only confirm the presence of these distinct Treg phenotypes in our study population, but also visualize the marker distribution which revealed that all HLA-DR$^+$, ICOS$^+$ and CD38$^+$ cells were found within the CTLA4$^+$ Treg subset. Similar to CD25 and GITR, CTLA4 is a T cell activation marker (10) and has been shown to correlate with FOXP3 expression in human CD4$^+$ T cells (45). Experimental models showed that CTLA4 is crucial for the suppressive function of Tregs through the modulation of APCs (30) and its interaction with CD80 and CD86 on conventional T cells (46).

Although Treg frequencies were not expanded in helminth infected individuals and no treatment-related change was seen, consistent with previous work in children from

the same study area (14, 15), the proportion of CTLA4$^+$ Tregs was significantly higher in helminth infected individuals and declined after treatment which is in line with previous reports (15, 47). Analysis at the cluster level revealed that the CTLA4$^+$ clusters in particular, often co-expressing ICOS and/or HLA-DR and/or CD38, were expanded in Indonesians compared to Europeans, indicating that helminths induce a particular Treg phenotype which could be represented by cells with increased regulatory capacity.

Besides Th2 cells and ILC2s being a source of type 2 cytokines, we identified Tc2 cells (type 2 cytokine-secreting CD8$^+$ T cells (33)) and a cluster of γδ T cells, which were capable of producing type 2 cytokines. Although Tc2 cells have recently been found to be enriched in patients with eosinophilic asthma (34), this subset has rarely been investigated, and therefore the current study is one of the first to characterize these cells in the context of human helminth infections.

Like Tc2 cells, not much is known about type 2 cytokine-producing γδ T cells, although their existence has been described before (48-52). Inagaki et al. showed a protective role of γδ T cells against infection with *N. brasiliensis* in mice, which was associated with the production of type 2 cytokines, in particular IL-13 (49). However, to our knowledge, the presence of type 2 cytokine-producing γδ T cells in human helminth infection has not been reported before. Here, we identified type 2 cytokine-producing γδ T cells, and showed that these cells were present in helminth-infected individuals, indicating their possible participation in the development of Th2 responses. However, further studies are required to investigate the function of Tc2 and type 2 cytokine-producing γδ T cells.

IL-10 producing B cells, known as regulatory B cells (Bregs), represent a relatively rare cell type within the human immune system that can suppress inflammatory responses (53). Although the frequency of IL-10 producing B cells was similar in Europeans and Indonesians and deworming did not affect their frequency, the phenotype of these cells was strikingly different with relatively more CD11c$^+$CD38$^-$, and less CD11c$^-$CD38$^+$ IL-10$^+$ B cells present in Indonesians. CD11c$^+$ B cells are increasingly recognized as a distinct population of memory B cells, and have been shown to expand in settings of chronic infections such as HIV, malaria and TB as well as in several autoimmune diseases (54, 55). In line with this, we found a significantly expanded population of CD11c$^+$Tbet$^+$ B cells in helminth-infected Indonesians compared to Europeans, of which a small fraction appeared capable of producing IL-10. Whereas CD38 has previously been reported as a marker for human Bregs (53), the expression of CD11c has not yet been associated with Bregs and further studies investigating the suppressive properties of CD11c$^+$IL-10$^+$ B cells will be needed.

Our study has a number of limitations. The small number of study subjects, the lack of placebo-treated individuals and the possibility that other infections are affected by deworming.

The work described here provided a detailed insight into the types of cells that participate in the strong type 2 and regulatory response induced by helminths. We demonstrate the advantage of using mass cytometry combined with HSNE, which allowed the identification of rare cell populations, such as ILC2s, Tc2 cells and Bregs, and provided

an opportunity to analyse the heterogeneity within Th2 cells and Tregs. Therefore this study forms the basis for the analysis of the identified cell subpopulations by flow cytometry in larger studies, not only in helminth infections, but also in other disease settings, as well as for their further functional characterization.

ACKNOWLEDGEMENTS

We would like to thank the volunteers who participated in this study. We would also like to thank all field workers from Universitas Indonesia and Nangapanda; Yvonne Kruize, Sanne de Jong and Astrid Voskamp for their help with the study. This work was supported by the Royal Netherlands Academy of Arts and Science (KNAW), Ref 57-SPIN3-JRP and Universitas Indonesia (Research Grant BOPTN 2742/H2.R12/HKP.05.00/2013.).

REFERENCES

1. Hotez PJ, Brindley PJ, Bethony JM, King CH, Pearce EJ, Jacobson J. Helminth infections: the great neglected tropical diseases. The Journal of clinical investigation **2008**; 118(4): 1311-21.
2. Maizels RM, Yazdanbakhsh M. Immune regulation by helminth parasites: cellular and molecular mechanisms. Nature reviews Immunology **2003**; 3(9): 733-44.
3. Allen JE, Wynn TA. Evolution of Th2 immunity: a rapid repair response to tissue destructive pathogens. PLoS pathogens **2011**; 7(5): e1002003.
4. de Ruiter K, Tahapary DL, Sartono E, et al. Helminths, hygiene hypothesis and type 2 diabetes. Parasite immunology **2017**; 39(5).
5. Moro K, Yamada T, Tanabe M, et al. Innate production of T(H)2 cytokines by adipose tissue-associated c-Kit(+)Sca-1(+) lymphoid cells. Nature **2010**; 463(7280): 540-4.
6. Neill DR, Wong SH, Bellosi A, et al. Nuocytes represent a new innate effector leukocyte that mediates type-2 immunity. Nature **2010**; 464(7293): 1367-70.
7. Price AE, Liang HE, Sullivan BM, et al. Systemically dispersed innate IL-13-expressing cells in type 2 immunity. Proceedings of the National Academy of Sciences of the United States of America **2010**; 107(25): 11489-94.
8. Mjosberg JM, Trifari S, Crellin NK, et al. Human IL-25- and IL-33-responsive type 2 innate lymphoid cells are defined by expression of CRTH2 and CD161. Nat Immunol **2011**; 12(11): 1055-62.
9. Simoni Y, Newell EW. Dissecting human ILC heterogeneity: more than just three subsets. Immunology **2018**; 153(3): 297-303.
10. Sakaguchi S, Miyara M, Costantino CM, Hafler DA. FOXP3+ regulatory T cells in the human immune system. Nature reviews Immunology **2010**; 10(7): 490-500.
11. Maizels RM, Smith KA. Regulatory T cells in infection. Adv Immunol **2011**; 112: 73-136.
12. Metenou S, Nutman TB. Regulatory T cell subsets in filarial infection and their function. Frontiers in immunology **2013**; 4: 305.
13. Watanabe K, Mwinzi PN, Black CL, et al. T regulatory cell levels decrease in people infected with Schistosoma mansoni on effective treatment. The American journal of tropical medicine and hygiene **2007**; 77(4): 676-82.
14. Wammes LJ, Hamid F, Wiria AE, et al. Regulatory T cells in human geohelminth infection suppress immune responses to BCG and Plasmodium falciparum. European journal of immunology **2010**; 40(2): 437-42.
15. Wammes LJ, Hamid F, Wiria AE, et al. Community deworming alleviates geohelminth-induced immune hyporesponsiveness. Proceedings of the National Academy of Sciences of the United States of America **2016**; 113(44): 12526-31.
16. van der Maaten L, Hinton G. Visualizing Data using t-SNE. J Mach Learn Res **2008**; 9: 2579-605.
17. McInnes L HJ. UMAP: Uniform Manifold Approximation and Projection for Dimension Reduction. https://arxivorg/pdf/180203426pdf **2018**.
18. Pezzotti N, Hollt T, Lelieveldt B, Eisemann E, Vilanova A. Hierarchical Stochastic Neighbor Embedding. Comput Graph Forum **2016**; 35(3): 21-30.
19. van Unen V, Hollt T, Pezzotti N, et al. Visual analysis of mass cytometry data by hierarchical stochastic neighbour embedding reveals rare cell types. Nature communications **2017**; 8(1): 1740.
20. Tahapary DL, de Ruiter K, Martin I, et al. Helminth infections and type 2 diabetes: a cluster-randomized placebo controlled SUGARSPIN trial in Nangapanda, Flores, Indonesia. BMC infectious diseases **2015**; 15: 133.
21. Tahapary DL, de Ruiter K, Martin I, et al. Effect of Anthelmintic Treatment on Insulin Resistance: A Cluster-Randomized, Placebo-Controlled Trial in Indonesia. Clin Infect Dis **2017**; 65(5): 764-71.
22. Wiria AE, Prasetyani MA, Hamid F, et al. Does treatment of intestinal helminth infections influence malaria? Background and methodology of a longitudinal study of clinical, parasitological and immunological parameters in Nangapanda, Flores, Indonesia (ImmunoSPIN Study). BMC infectious diseases **2010**; 10: 77.
23. Hollt T, Pezzotti N, van Unen V, et al. Cytosplore: Interactive Immune Cell

Phenotyping for Large Single-Cell Datasets. Comput Graph Forum **2016**; 35(3): 171-80.
24. Comaniciu D, Meer P. Mean shift: A robust approach toward feature space analysis. Ieee T Pattern Anal **2002**; 24(5): 603-19.
25. Beyrend G, Stam K, Hollt T, Ossendorp F, Arens R. *Cytofast*: A workflow for visual and quantitative analysis of flow and mass cytometry data to discover immune signatures and correlations. Computational and Structural Biotechnology Journal **2018**.
26. Cosmi L, Annunziato F, Galli MIG, Maggi RME, Nagata K, Romagnani S. CRTH2 is the most reliable marker for the detection of circulating human type 2 Th and type 2 T cytotoxic cells in health and disease. European journal of immunology **2000**; 30(10): 2972-9.
27. Mitson-Salazar A, Prussin C. Pathogenic Effector Th2 Cells in Allergic Eosinophilic Inflammatory Disease. Front Med (Lausanne) **2017**; 4: 165.
28. Mahnke YD, Brodie TM, Sallusto F, Roederer M, Lugli E. The who's who of T-cell differentiation: human memory T-cell subsets. European journal of immunology **2013**; 43(11): 2797-809.
29. Simoni Y, Fehlings M, Kloverpris HN, et al. Human Innate Lymphoid Cell Subsets Possess Tissue-Type Based Heterogeneity in Phenotype and Frequency. Immunity **2017**; 46(1): 148-61.
30. Wing K, Onishi Y, Prieto-Martin P, et al. CTLA-4 control over Foxp3+ regulatory T cell function. Science (New York, NY) **2008**; 322(5899): 271-5.
31. Pesenacker AM, Bending D, Ursu S, Wu Q, Nistala K, Wedderburn LR. CD161 defines the subset of FoxP3+ T cells capable of producing proinflammatory cytokines. Blood **2013**; 121(14): 2647-58.
32. Afzali B, Mitchell PJ, Edozie FC, et al. CD161 expression characterizes a subpopulation of human regulatory T cells that produces IL-17 in a STAT3-dependent manner. European journal of immunology **2013**; 43(8): 2043-54.
33. Seder RA, Le Gros GG. The functional role of CD8+ T helper type 2 cells. J Exp Med **1995**; 181(1): 5-7.
34. Hilvering B, Hinks TSC, Stoger L, et al. Synergistic activation of pro-inflammatory type-2 CD8(+) T lymphocytes by lipid mediators in severe eosinophilic asthma. Mucosal Immunol **2018**.
35. Brodin P, Jojic V, Gao T, et al. Variation in the human immune system is largely driven by non-heritable influences. Cell **2015**; 160(1-2): 37-47.
36. Boyd A, Ribeiro JM, Nutman TB. Human CD117 (cKit)+ innate lymphoid cells have a discrete transcriptional profile at homeostasis and are expanded during filarial infection. PloS one **2014**; 9(9): e108649.
37. Nausch N, Appleby LJ, Sparks AM, Midzi N, Mduluza T, Mutapi F. Group 2 innate lymphoid cell proportions are diminished in young helminth infected children and restored by curative anti-helminthic treatment. PLoS neglected tropical diseases **2015**; 9(3): e0003627.
38. Spits H, Artis D, Colonna M, et al. Innate lymphoid cells--a proposal for uniform nomenclature. Nature reviews Immunology **2013**; 13(2): 145-9.
39. Lim AI, Li Y, Lopez-Lastra S, et al. Systemic Human ILC Precursors Provide a Substrate for Tissue ILC Differentiation. Cell **2017**; 168(6): 1086-100 e10.
40. Mitson-Salazar A, Yin Y, Wansley DL, et al. Hematopoietic prostaglandin D synthase defines a proeosinophilic pathogenic effector human T(H)2 cell subpopulation with enhanced function. The Journal of allergy and clinical immunology **2016**; 137(3): 907-18 e9.
41. Anuradha R, George PJ, Hanna LE, et al. Parasite-antigen driven expansion of IL-5(-) and IL-5(+) Th2 human subpopulations in lymphatic filariasis and their differential dependence on IL-10 and TGFbeta. PLoS neglected tropical diseases **2014**; 8(1): e2658.
42. Baecher-Allan C, Wolf E, Hafler DA. MHC class II expression identifies functionally distinct human regulatory T cells. Journal of immunology (Baltimore, Md : 1950) **2006**; 176(8): 4622-31.
43. Ito T, Hanabuchi S, Wang YH, et al. Two functional subsets of FOXP3+ regulatory T cells in human thymus and periphery. Immunity **2008**; 28(6): 870-80.
44. Patton DT, Wilson MD, Rowan WC, Soond DR, Okkenhaug K. The PI3K p110delta regulates expression of CD38 on regulatory T cells. PloS one **2011**; 6(3): e17359.
45. Yagi H, Nomura T, Nakamura K, et al. Crucial role of FOXP3 in the development and function of human CD25+CD4+ regulatory T cells. Int Immunol **2004**; 16(11): 1643-56.
46. Paust S, Lu L, McCarty N, Cantor H. Engagement of B7 on effector T cells by regulatory T cells prevents autoimmune disease. Proceedings of the National Academy of Sciences of the United States of America **2004**; 101(28): 10398-403.
47. Garcia-Hernandez MH, Alvarado-Sanchez B, Calvo-Turrubiartes MZ, et al. Regulatory T Cells in children with intestinal parasite infection. Parasite immunology **2009**; 31(10): 597-603.
48. Ferrick DA, Schrenzel MD, Mulvania T, Hsieh B, Ferlin WG, Lepper H. Differential production of interferon-gamma and interleukin-4 in response to Th1- and Th2-stimulating pathogens by gamma delta T cells in vivo. Nature **1995**; 373(6511): 255-7.
49. Inagaki-Ohara K, Sakamoto Y, Dohi T, Smith AL. gammadelta T cells play a protective role during infection with Nippostrongylus brasiliensis by promoting goblet cell function in the small intestine. Immunology **2011**; 134(4): 448-58.
50. Zuany-Amorim C, Ruffie C, Haile S, Vargaftig BB, Pereira P, Pretolani M. Requirement for gammadelta T cells in allergic airway inflammation. Science (New York, NY) **1998**; 280(5367): 1265-7.
51. Spinozzi F, Agea E, Bistoni O, et al. Increased allergen-specific, steroid-sensitive gamma delta T cells in bronchoalveolar lavage fluid from patients with asthma. Ann Intern Med **1996**; 124(2): 223-7.
52. Krug N, Erpenbeck VJ, Balke K, et al. Cytokine profile of bronchoalveolar lavage-derived CD4(+), CD8(+), and gammadelta T cells in people with asthma after segmental allergen challenge. American journal of respiratory cell and molecular biology **2001**; 25(1): 125-31.
53. Mauri C, Menon M. The expanding family of regulatory B cells. Int Immunol **2015**; 27(10): 479-86.
54. Karnell JL, Kumar V, Wang J, Wang S, Voynova E, Ettinger R. Role of CD11c(+) T-bet(+) B cells in human health and disease. Cellular immunology **2017**; 321: 40-5.
55. Winslow GM, Papillion AM, Kenderes KJ, Levack RC. CD11c+ T-bet+ memory B cells: Immune maintenance during chronic infection and inflammation? Cellular immunology **2017**; 321: 8-17.

SUPPLEMENTAL DATA

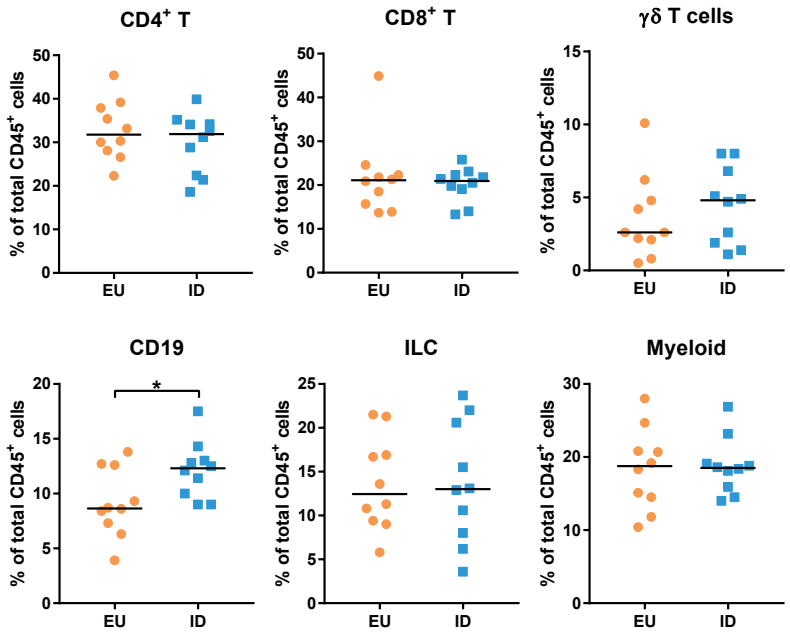

Supplementary Figure S1. Lineage frequencies. Scatterplots comparing lineage frequencies of Europeans (EU) and Indonesians (ID). Median is shown. Differences between EU and ID Pre were tested with Student's t-test. *P <.05.

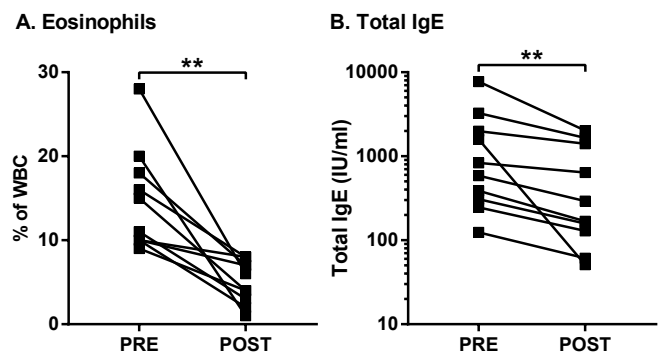

Supplementary Figure S2. Eosinophil counts and total IgE levels. A. Eosinophil counts expressed as percentage of white blood cells (WBC) and **B.** Serum levels of total IgE of Indonesians pre- and post-anthelmintic treatment. **P <.01.

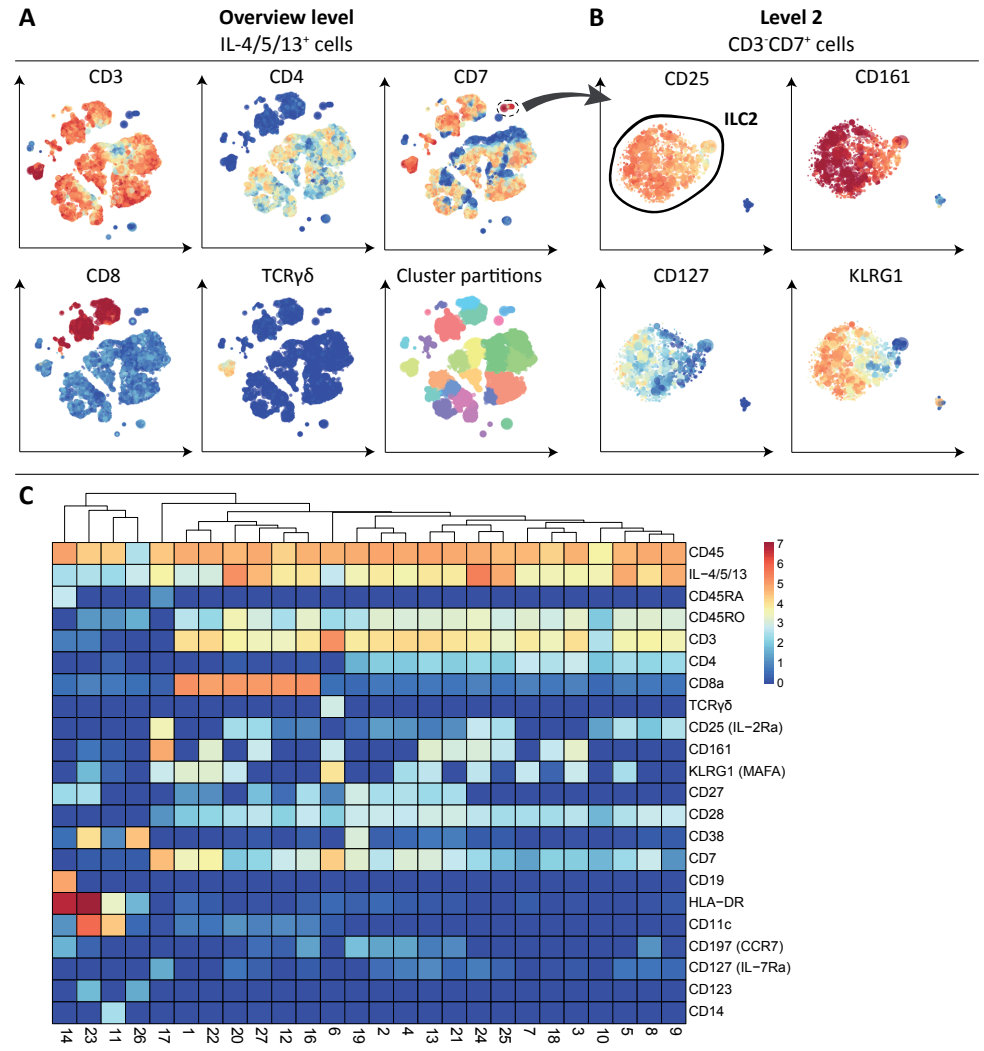

Supplementary Figure S3. Type 2-cytokine producing cells. A. First level embedding of IL-4/5/13$^+$ cells clustered on surface markers and cluster partitions of IL-4/5/13$^+$ cells using GMS clustering (lower right panel). The expression of CD4 was reduced as a consequence of the stimulation. Colour represents arsin5-transformed marker expression as indicated. Size of the landmarks represents AoI. **B.** Second level embedding of the CD3$^-$CD7$^+$ landmarks selected from the first level in a, as indicated by the black encirclement, allowed the identification of ILC2s. **C.** A heatmap summary of median expression values of cell markers expressed by IL-4/5/13$^+$ cells identified in a. and hierarchical clustering thereof.

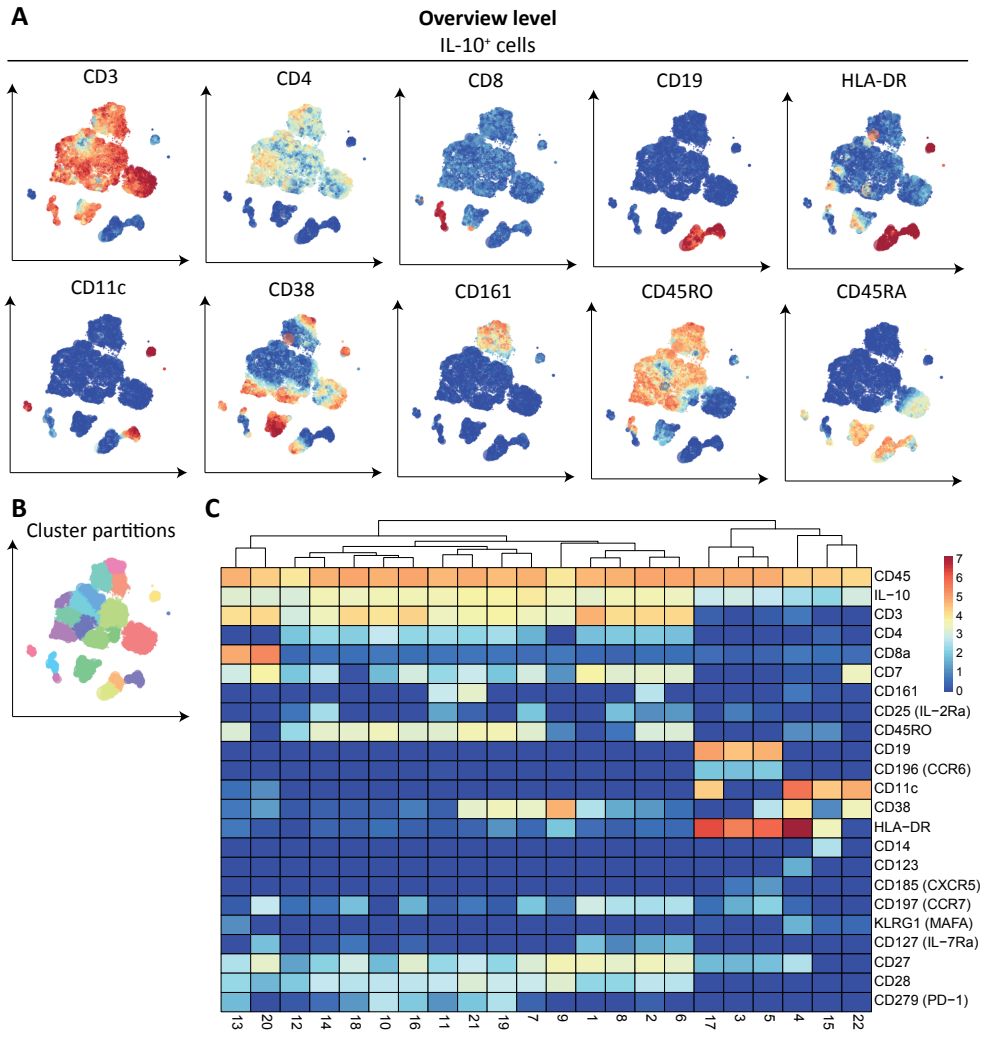

Supplementary Figure S4. IL-10 producing cells. A. First level embedding of IL-10⁺ cells clustered on surface markers. The expression of CD4 was reduced as a consequence of the stimulation. Colour represents arsin5-transformed marker expression as indicated. Size of the landmarks represents AoI. **B.** Cluster partitions of IL-10⁺ cells using GMS clustering. **C.** A heatmap summary of median expression values of cell markers expressed by IL-10⁺ cells identified in b. and hierarchical clustering thereof.

Supplementary table S1. Antibody panel 1 (Phenotyping).

Label	Specificity	Clone	Vendor	Catalogue number	Dilution
^{89}Y	CD45	HI30	Fluidigm[a]	3089003B	200x
^{113}CD	CD45RA	HI100	eBioscience[b]	83-0458-42	50x
^{141}Pr	CD196 (CCR6)	G034E3	Fluidigm	3141003A	100x
^{142}Nd	CD19	HIB19	Fluidigm	3142001B	200x
^{143}Nd	CD117 (c-Kit)	104D2	Fluidigm	3143001B	100x
^{145}Nd	CD4	RPA-T4	Fluidigm	3145001B	100x
^{146}Nd	CD8a	RPA-T8	Fluidigm	3146001B	200x
^{147}Sm	CD183 (CXCR3)	G025H7	BioLegend[c]	353733	100x
^{148}Nd	CD14	M5E2	BioLegend	301843	100x
^{149}Sm	CD25 (IL-2Ra)	2A3	Fluidigm	3149010B	100x
^{150}Nd	CD185 (CXCR5)	J252D4	BioLegend	356902	100x
^{151}Eu	CD123	6H6	Fluidigm	3151001B	100x
^{152}Sm	TCRγδ	11F2	Fluidigm	3152008B	50x
^{153}Eu	CD7	CD7-6B7	Fluidigm	3153014B	100x
^{154}Sm	CD163	GHI/61	Fluidigm	3154007B	100x
^{155}Gd	CD278 (ICOS)	C398.4A	BioLegend	313502	50x
^{156}Gd	CD294 (CRTH2)	BM16	BioLegend	350102	50x
^{158}Gd	CD122 (IL-2Rb)	TU27	BioLegend	339015	100x
^{159}Tb	CD197 (CCR7)	G043H7	Fluidigm	3159003A	100x
^{160}Gd	FOXP3	PCH101	eBioscience	14-4776-82	50x
^{161}Dy	KLRG1 (MAFA)	REA261	Miltenyi[d]	Special order	100x
^{162}Dy	CD11c	Bu15	Fluidigm	3162005B	200x
^{163}Dy	CD152 (CTLA-4)	BNI3	BioLegend	369602	100x
^{164}Dy	CD161	HP-3G10	Fluidigm	3164009B	100x
^{165}Ho	CD127 (IL-7Rα)	AO19D5	Fluidigm	3165008B	200x
^{166}Er	Tbet	4B10	BioLegend	644825	50x
^{167}Er	CD27	O323	Fluidigm	3167002B	200x
^{168}Er	HLA-DR	L243	BioLegend	307651	200x
^{169}Tm	GATA3	REA174	Miltenyi	130-108-061	50x
^{170}Er	CD3	UCHT1	Fluidigm	3170001B	100x
^{171}Yb	CD28	CD28.2	BioLegend	302937	200x
^{172}Yb	CD38	HIT2	Fluidigm	3172007B	200x
^{173}Yb	CD45RO	UCHL1	BioLegend	304239	100x
^{174}Yb	CD335 (NKp46)	92E	BioLegend	331902	100x
^{175}Lu	CD279 (PD-1)	EH 12.2H7	Fluidigm	3175008B	100x
^{176}Yb	CD56	NCAM16.2	Fluidigm	3176008B	100x
^{209}Bl	CD16	3G8	Fluidigm	3209002B	400x

[a]Fluidigm, South San Francisco, CA, USA. [b]eBioscience, San Diego, CA, USA. [c]Biolegend, San Diego, CA, USA. [d]Miltenyi Biotech, Bergisch Gladbach, Germany. CCR, C-C chemokine receptor. CD, cluster of differentiation. CRTH2, prostaglandin D2 receptor 2. CXCR, CXC chemokine receptor. FOXP3, forkhead box P3. HLA-DR, human leukocyte antigen-D-related. IL-2R, interleukin-2 receptor. IL-7Rα, interleukin-7 receptor α. KLRG1, killer cell lectin-like receptor subfamily G member 1. MAFA, mast cell function-associated antigen. PD-1, programmed cell death protein. TCR, T-cell receptor. Markers in grey were stained intranuclear, while all other markers were stained on the cell surface.

Supplementary table S2. Antibody panel 2 (Cytokine production).

Label	Specificity	Clone	Vendor	Catalogue number	Dilution
^{89}Y	CD45	HI30	Fluidigm[a]	3089003B	200x
^{113}CD	CD45RA	HI100	Ebioscience[b]	83-0458-42	50x
^{141}Pr	CD196 (CCR6)	G034E3	Fluidigm	3141003A	100x
^{142}Nd	CD19	HIB19	Fluidigm	3142001B	200x
^{143}Nd	CD117 (c-Kit)	104D2	Fluidigm	3143001B	100x
^{144}Nd	IL-2	MQ117H12	BioLegend[c]	500339	400x
^{145}Nd	CD4	RPA-T4	Fluidigm	3145001B	100x
^{146}Nd	CD8a	RPA-T8	Fluidigm	3146001B	200x
^{147}Sm	CD183 (CXCR3)	G025H7	BioLegend	353733	100x
^{148}Nd	CD14	M5E2	BioLegend	301843	100x
^{149}Sm	CD25 (IL-2Ra)	2A3	Fluidigm	3149010B	100x
^{150}Nd	CD185 (CXCR5)	J252D4	BioLegend	356902	100x
^{151}Eu	CD123	6H6	Fluidigm	3151001B	100x
^{152}Sm	TCRγδ	11F2	Fluidigm	3152008B	50x
^{153}Eu	CD7	CD7-6B7	Fluidigm	3153014B	100x
^{154}Sm	CD163	GHI/61	Fluidigm	3154007B	100x
^{155}Gd	IFNγ	B27	BioLegend	506521	400x
^{156}Gd	CD294 (CRTH2)	BM16	BioLegend	350102	50x
^{158}Gd	CD122 (IL-2Rb)	TU27	BioLegend	339015	100x
^{159}Tb	CD197 (CCR7)	G043H7	Fluidigm	3159003A	100x
^{160}Gd	TNFα	MAb11	BioLegend	502941	400x
^{161}Dy	KLRG1 (MAFA)	REA261	Miltenyi[d]	Special order	100x
^{162}Dy	CD11c	Bu15	Fluidigm	3162005B	200x
^{163}Dy	IL-17	BL168	BioLegend	512331	400x
^{164}Dy	CD161	HP-3G10	Fluidigm	3164009B	100x
^{165}Ho	CD127 (IL-7Ra)	AO19D5	Fluidigm	3165008B	200x
^{166}Er	IL-10	JES39D7	Fluidigm	3166008B	400x
^{167}Er	CD27	O323	Fluidigm	3167002B	200x
^{168}Er	HLA-DR	L243	BioLegend	307651	200x
^{169}Tm	IL-4	MP4-25D2	Fluidigm	3169016B	400x
^{169}Tm	IL-5	TRFK5	BioLegend	500829	400x
^{169}Tm	IL-13	JES105A2	BioLegend	504309	400x
^{170}Er	CD3	UCHT1	Fluidigm	3170001B	100x
^{171}Yb	CD28	CD28.2	BioLegend	302937	200x
^{172}Yb	CD38	HIT2	Fluidigm	3172007B	200x
^{173}Yb	CD45RO	UCHL1	BioLegend	304239	100x
^{175}Lu	CD279 (PD-1)	EH 12.2H7	Fluidigm	3175008B	100x
^{176}Yb	CD56	NCAM16.2	Fluidigm	3176008B	100x

[a]Fluidigm, South San Francisco, CA, USA. [b]eBioscience, San Diego, CA, USA. [c]Biolegend, San Diego, CA, USA. [d]Miltenyi Biotech, Bergisch Gladbach, Germany. CCR, C-C chemokine receptor. CD, cluster of differentiation. CRTH2, prostaglandin D2 receptor 2. CXCR, CXC chemokine receptor. HLA-DR, human leukocyte antigen-D-related. IL-2R, interleukin-2 receptor. IL-7Rα, interleukin-7 receptor α. KLRG1, killer cell lectin-like receptor subfamily G member 1. MAFA, mast cell function-associated antigen. PD-1, programmed cell death protein. TCR, T-cell receptor. Markers in grey were stained intracellular, while all other markers were stained on the cell surface.